Journal of Scientific & Industrial Research
Vol. 83, March 2024, pp. 264-273
DOI: 10.56042/jsir.v83i3.1498

Retinal Blood Vessel Segmentation through Morphology Cascaded Features and Supervised Learning

Y Aruna Suhasini Devi[1]* & Manjunatha Chari Kamsali[2]
[1]Department of ECE, CMR College of Engineering & Technology, Hyderabad 501 401, Telangana, India
[2]Department of EECE, GITAM University, Hyderabad 502 329, Telangana, India

Received 14 May 2023; revised 26 January 2024; accepted 12 February 2024

Retinal blood vessels are the most important attributes in the automatic diagnosis of Diabetic Retinopathy (DR). Since the advanced stages of DR are diagnosed through blood vessels, their segmentation followed by clear analysis is required. Such process can be accompanied through the classification. Segmentation of minor and thin vessels is a challenge because they are analogous to background pixels in fundus image. To solve this issue, this paper proposes a three-stage retinal vessel segmentation mechanism from fundus images. In the first stage, the fundus image is pre-processed for enhancement and then major blood vessels are processed, after extracting them through filtering and morphological transformation. Each pixel of the resulting image is represented by a set of composite features and then processed for pixel level classification. A total of five different features are used to signify each pixel and then for classification Support Vector Machine (SVM) algorithm is used. In the final and post-processing stage, the outputs of first two stages are fused to get the complete retinal vessel structure. Using DRIVE dataset, the proposed method's experimental validation proves the effectiveness of segmentation accuracy and computational time. The average improvement in the Accuracy, Specificity and Sensitivity is observed as 2.3645%, 1.3365% and 5.2314% respectively from past recent vessel segmentation methods.

Keywords: Classification, Feature extraction, Minor vessels, Morphology, Post processing

Introduction

Recently, the eye related diseases like vein occlusions, macular edema, Diabetic Retinopathy (DR) and Glaucoma are found to be major and primary cause of blindness in people around the world.[1] Among these diseases, the DR plays major role as most of the people suffer from diabetes throughout the world. From recent studies,[2,3] the approximated number of DR patients was 126.6 million in the year of 2011, and it is approximated to rise to 191 million by 2030. Further, this number is estimated to grow furiously with the rise in the number of diabetic patients. To control this issue, an early-stage diagnosis of diabetic condition is a better solution. Retinal images are the main sources through which the DR diagnosis can be done. With the chronicity of diabetes, blood vessels in the retina get occluded, leading to new vessel formation. Such anomalies cause fluid to leak resulting in blurred vision. DR has no initial symptoms that can be identified at the initial stages. But there exist some symptoms like variations in the retinal vessel's structure, proliferation of new and abnormal retinal vessels, retina associated with fatty deposits and macula swelling that signify the presence of DR.[4] These symptoms can be detected through the study and analysis of the retinal vessel's characteristics like width, length, tortuosity, and branches that spread out in retinal image. Hence, segmentation and analysis of blood vessels is required which is a challenging task and consumes much time of experts for diagnosis. Since manual segmentation of blood vessels results in inaccurate diagnosis, automatic segmentation and analysis has gained significant attention in research.

Several methods were previously developed for the detection of Non-proliferative DR (NPDR). For example, two studies[5,6] used masking to extract the retinal vasculature. These methods guarantee the correct classification of pixels of retinal vessels from the pixels of red lesions which incur due to the presence of DR. In case of Proliferative DR (PDR), the blood vessel's segmentation from retinal images requires the analysis of vessel width, density and the tortuosity of blood vessels. An accurate and fast automated segmentation mechanism is required that can help in the perfect diagnosis of DR related issues. Some earlier methods have gained an accuracy of

*Author for Correspondence
E-mail: arunasuha@gmail.com

92% on normal retinal images through the template matching and line detection methods.[7,8] These are computationally much faster but they are unable to attain high accuracy in the case of retinal images with DR abnormalities like red lesions (Microaneurysms and hemorrhages) or bright lesions (Cotton Wool Spots and Exudates), or illumination and contrast variations. Such situations result in complexity as pixels are considered directly.

To address these issues, a new vessel segmentation mechanism consisting of three stages is proposed in this paper. The 1st stage concentrates on the segmentation of major blood vessels. In the second phase, each pixel of the resulting image is characterized by feature vector of size 18-D and then subjected to pixel-based classification. For feature extraction, five different sets of features used, are Gradient, Hessian, statistical, Morphological and Edge. Finally, the significant contributions of the paper are presented as mentioned below.

1. To reduce the number of pixels for classification, the major vessels are segmented from retinal image based on mathematical morphology and low pass filtering, which in turn reduces the maximum complexity.
2. To achieve good classification accuracy of minor vessels, new composite features are used based on different sets of features. All these features are independent in nature and provide better discrimination between background and minor vessels.

Literature Survey

Automatic Segmentation of Retinal Blood Vessel from fundus images is essential for diagnosis of diseases like DR, Glaucoma, Macula Edema and Hypertension. With an increase in the number of DR cases, the research on retinal vessel segmentation has also increased and different researchers proposed different methods.

Zhu *et al.*[9] proposed 39-D feature vector to represent every pixel of retinal image and applied "Extreme Learning Machine (ELM)" for classification. The feature vector was formulated with the help of five different sets of features, which are Local features, Morphological features, Phase congruency, Hessian features and Divergence of Vectors fields. For simulation purposes, they used two benchmark databases namely DRIVE and "Retinal Images for Screening (RIS)".

Dash & Bhoi[10] proposed an unsupervised recursive method for the retinal blood vessel extraction from fundus images. Initially, they focused on contrast enhancement, and it was done through Gamma Correction and "Contrast Limited Adaptive Histogram Equalization (CLAHE)". Next, the retinal vessels were determined in an iterative fashion by employing adaptive thresholding for every iteration. To produce the final segmented image, they applied morphological cleaning operation. At the simulation experiments, they used two benchmark databases namely DRIVE and CHASE_DB1

Yan *et al.*[11] introduced a three-stage deep learning strategy to segment the minor as well as major blood vessels from fundus image. The three stages are namely, thick and darker blood vessel segmentation, thin and finer blood vessel segmentation and fusion. For the provision of better discrimination, they minimized the negative effect caused due to their high imbalance ratio. The final fusion separates the vessel pixels from non-vessel pixels and improves the consistency. CHASE_DB, STARE and DRIVE database were used for experimental validation.

Sazak *et al.*[12] focused on the retinal blood vessels segmentation and proposed a mathematical morphology assisted multi-scale vessel enhancement method called "Bowler-Hat Transform (BHT)". BHT combines multiple structuring elements to identify the vessel like structures. Khan *et al.*[13] proposed a specialized filter to increase the performance of computer aided diagnosis in low contrast retinal images.

Lin *et al.*[14] proposed the "Holistically Nested Edge Detector (HED)" after combining it with the conditional random field assisted global smoothness regularization along with deep supervision for the purpose of automatic retinal vasculature segmentation. This is a deep convolutional network-based method, and it is much more effective than the Conditional Random Fields (CRF) based methods and HED based methods. CHASE_DB1, STARE and DRIVE databases were used for experimental validation.

Tamim *et al.*[15] employed "Multilayer Perceptron Neural Network (MLPNN)" for the segmentation of blood vessels from funds image. At first, they described each pixel of funds image with a feature vector of size 24-D which is a composite form of five different features. They are Local Intensity, Morphological features, Phase congruency, Hessian

features and Difference of Gaussian features. In addition, they also employed mathematical morphology for post-processing to get optimized results at segmentation process. Three benchmark databases namely CHASE_DB1, STARE and DRIVE databases were used for experimental validation.

Kushol *et al.*[16] employed "Bendlet Transform (BT)" for extraction of vascular structure from fundus images. BT is regarded as a kind of wavelet transform that can help in acquiring the directional features which are not possible with traditional wavelet filters. Next, for classification, they employed an ensemble algorithm and validated the methodology through STARE and DRIVE databases.

Orujov *et al.*[17] applied Fuzzy Logic Rules based on Mamdani strategy for segmenting the vascular structure in the retinal images. In the initial stages, they employed CLAHE for contrast adjustment and Median filter for the background exclusion. Next, they determined the edges of blood vessels by applying fuzzy rules over the quality enhanced fundus image. Three benchmark databases namely DRIVE, CHASE_DB1 and STARE databases were used for experimental validation.

Shukla *et al.*[18] introduced a new "Fractional Filter (FF)"and "Eigen Value Map (EVM)" of local covariance matrix to segment retinal blood vessels. Design of the fractional filter is based on the exponential weight factor and Weighted Fractional Derivative. The covariance matrix is modeled based on the 2nd order moments of the image. STARE and DRIVE databases were used for validation.

Tchinda *et al.*[19] proposed "Classical Edge Detection Filters and Artificial Neural Networks (ANNs)" to segment blood vessels from fundus image. Different filters were applied to extract features and for classifying the pixel as either vessel or non-vessel, ANN was employed. CHASE, STARE and DRIVE databases were used for simulation experiments. Dikkala *et al.*[20] applied morphology preceded by noise cancellation and contrast enhancement for the purpose of feature extraction from fundus images.

Problem: Even though pixel-based classification methods have gained better accuracy, they are susceptible to different effects like red lesions, low contrasts, pathologies due to abnormalities. All these factors are less addressed in the previous methods. Hence, they had shown limited segmentation performance especially for low quality images.

Proposed Method

Overview

The proposed method explains in this section the details of blood vessels segmentation from fundus retinal images. The proposed approach is comprised of three stages; initially major blood vessels are extracted, then the classification of minor blood vessels is done and finally post processing is done. The presence of Minor vessels indicates severe DR, hence segmentation of entire retinal blood vessels (i.e., both minor and major) becomes very essential. Therefore, major blood vessels are processed for segmentation in the initial stage. Next the resulting image is processed for pixel level classification through composite feature extraction and supervised learning. At this stage, a different set of features were used to represent the characteristics of vessel pixels. After the completion of two stages, post processing is employed to get the final vessel structure. Post processing employs the fusion operation between the outputs obtained in the first two stages. The working of proposed blood vessel segmentation mechanism is depicted in Fig. 1.

Major Blood Vessels Extraction

The 1st stage of the proposed approach involves the extraction of major blood vessels from fundus image. Initially, the original color retinal image is processed for green plane extraction followed by contrast adjustment. Since the retinal image's Green channel clearly visualizes the DR attributes, it is only used for further processing. For contrast enhancement "Spatial Collaboration Contrast Enhancement (SCCE)",[21] is applied. As the retinal vessels are darker than a non-vessel region, contrast enhancement makes them darker such that the extraction becomes more effective. After the contrast enhancement, the resultant image is applied for noise removal through median filtering. Then the enhanced image is subjected to normalization and all the pixel values are normalized into a range of 0 to 1. Consider the I_E to be the enhanced image, it is normalized as

$$I_N(x,y) = \frac{I_E(x,y)}{\max(I_E)}, \forall (x,y) \in [M\ N] \quad \ldots (1)$$

where, $I_E(x,y)$ is the white pixel value in enhanced image and $\max(I_E)$ is the maximum pixel intensity in contrast enhanced image. Once the normalization is completed, then it is subjected to major blood vessels extraction in two phases. In the first phase, the green plane is subjected to the major blood vessel extraction

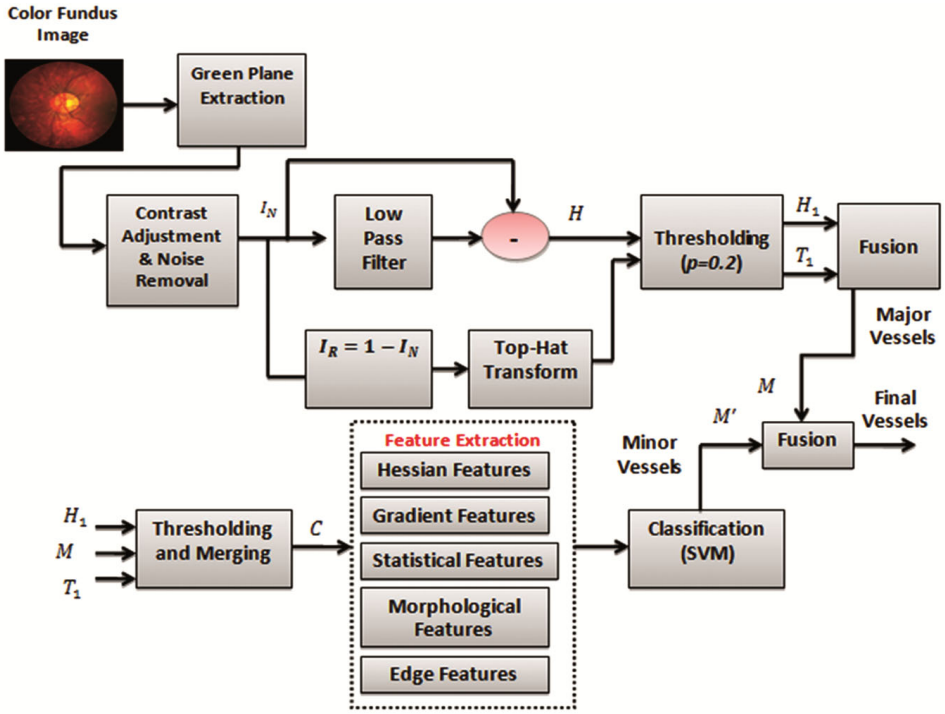

Fig. 1 — Overall working schematic of proposed segmentation method

while in the second phase; the negative of green plane, i.e., red plane is subjected to major blood vessels extraction.

In the first phase, the I_N is smoothened through a Low Pass Filter (LPF) and then subtracted from the absolute I_N. After the completion of subtraction, the output obtained is called as High Pass Filter (HPF) image after thresholding it against zero. Mathematically the high pass filter image is obtained as[22]

$$H(x,y) = abs(I_N(x,y) - LPF(I_N(x,y)) > 0) \quad \ldots (2)$$

For the accomplishment of LPF, median filter is applied by keeping the window size as 20×20.[23] After getting a threshold image, it is subjected to contrast adjustment to get the regions of vessels. Then the $H(x,y)$ is thresholded against threshold p to get the binary image and let it be H_1. At this phase, the threshold value is set as $p = 0.2$ and the pixel value whose intensity is greater than 0.2 is assigned to 1 otherwise it is assigned to 0. The thresholding operation is mathematically derived as

$$H_1(x,y) = \begin{cases} 1; if\ H(x,y) > p \\ 0;\ Otherwise \end{cases} \quad \ldots (3)$$

In the second phase, the proposed segmentation mechanism considers the negative version of normalized image for the extraction of vessels from dark regions and let the resultant image be denoted as I_R. Next I_R is subjected to top-hat transform[24] to get totally 12 top-hat reconstructions.

For each reconstruction the length of linear structuring element is kept as 15 pixels and width is kept as 1. The angular deviation maintained between each reconstruction is 15° and it starts from 0° and ends in 180°. The main reason for selection of linear structuring element of length 15 is to extract even the biggest retinal vessels. After reconstruction, the final image is constructed by choosing the maximum intensity value out of 12 reconstructions. Top-hat reconstruction is done according to the following equations.

$$I_R = (1 - I_N) \circ g \quad \ldots (4)$$

$$T_{i,i=1\ to\ 12} = Top - Hat(I_R^{\theta}), \theta = 0^{\circ}:15^{\circ}:180^{\circ} \quad \ldots (5)$$

$$T(x,y) = \max(T_i), i = 1\ to\ 12 \quad \ldots (6)$$

After obtaining T, it was subjected to a thresholding process against p. Here the value of p is chosen as 0.2. In the equation for T, the pixel is assigned 1 if its intensity is greater than 0.2 otherwise it is assigned 0 and final image obtained is a binary image.

$$T_1(x,y) = \begin{cases} 1; if\ T(x,y) > p \\ 0;\ Otherwise \end{cases} \quad \ldots (7)$$

Once the vessel binary images are obtained, they are subjected to fusion process to get the regions of major blood vessels and are simply called as major blood vessel image and let it be denoted as M. For fusion process intersection operation is employed which results in pixels with common values. The final measure of blood vessel image is obtained as

$$M(x,y) = \begin{cases} 1; if\ H_1(x,y) = T_1(x,y) = 1 \\ 0;\ Otherwise \end{cases} \quad (or) \quad M = H_1 \cap T_1 \quad \ldots (8)$$

The resultant M is an image with major blood vessels which are very important regions for the diagnosis of DR.

Minor Blood Vessels Extraction

After the removal of major vessels from the two binary images such as H_1 and T_1 the resultant image is simply called as minor vessel images and let it be denoted as H_1' and T_1'. The determination of H_1' and T_1' is done according to the following equation.[22]

$$H_1^{'} = \begin{cases} 1; if\ M(x,y) = 0\ and\ H_1(x,y) = 1 \\ 0;\ Otherwise \end{cases} \quad \ldots (9)$$

And

$$T_1^{'} = \begin{cases} 1; if\ M(x,y) = 0\ and\ T_1(x,y) = 1 \\ 0;\ Otherwise \end{cases} \quad \ldots (10)$$

For the second stage, three images are considered as inputs such as M, H_1 and T_1. From M and H_1 one minor vessel image is derived, i.e., H_1' and from M and T_1 another minor vessel image is derived, i.e., T_1'. Next H_1' and T_1' are used to produce a common Minor vessel image and let it be denoted as C, mathematically it is derived as

$$C(x,y) = \begin{cases} 1; if\ H_1^{'}(x,y) = 1\ and\ T_1^{'}(x,y) = 1 \\ 0;\ Otherwise \end{cases} \quad \ldots (11)$$

Next the common Minor vessel image is processed for classification at pixel level. This classification is done under two stages, i.e., feature extraction followed by classification.

Feature Extraction

Here, the proposed approach uses five different filters to extract several features from resultant image. They are namely Morphological features, Statistical features, Edge features, Gradient and Hessian features which are as mentioned below.

Gradient Feature: Scalar field's directional derivative is known as a gradient. The gradient provides the details contained in the image. The image gradients are calculated in both vertical and horizontal directions. Based on these two gradients, the magnitude and direction of final gradient are measured. Each pixel is represented with four gradient features, they are G_x, G_y, G_M and G_θ. G_M is called as Gradient magnitude and G_θ is called as gradient direction, they are calculated as follows.

$$G_\theta(x,y) = \tan^{-1}\left(\frac{G_y(x,y)}{G_x(x,y)}\right) \quad \ldots (12)$$

$$G_M(x,y) = \sqrt{\left(G_x(x,y)\right)^2 + \left(G_y(x,y)\right)^2} \quad \ldots (13)$$

where, $G_y(x,y)$ and $G_x(x,y)$ are the two gradients along two directions such as x- and y-axis. They are computed as follows.

$$G_y(x,y) = |C(x,y+1) - C(x,y-1)| \quad \ldots (14)$$

$$G_x(x,y) = |C(x+1,y) - C(x-1,y)| \quad \ldots (15)$$

Difference between successive pixels and $G_\theta(x,y)$ are explored and the direction of the resultant pixel movement is determined.

Hessian Features: Generally, a multivariable function's 2nd order derivative is used to construct Hessian matrix. As it is flexible, the blood vessels structural features are easily acquired. Each pixel is represented using three features to determine the Hessian features, as represented in Eq. (16).

$$H = \begin{bmatrix} G_{xx} & G_{xy} \\ G_{yx} & G_{yy} \end{bmatrix} \quad \ldots (16)$$

where, G_{xx} and G_{yy} are the gradients of 2nd order along x and y-directions respectively. G_{xy} is termed as the dependent gradient along x-direction with reference to y parameter and G_{yx} is termed as the dependent gradient along y-direction with reference to x parameter. These 2nd order gradients help in the determination of minor blood vessels from resultant image.

Statistical Features: The statistical features normally explore the statistical means of values in the pixel-based classification. Since blood vessels differ from image to image, these features help in exploring the

statistical variations. These features are calculated by considering 8 features for each pixel. The nominee pixel is located at the center of window, whose size is set as 21 × 21.[25] A total of 8 features are measured for every window, they are Mean, Maximum, "Mean Absolute Deviation (MAD)", Minimum, Standard deviation, "Root Sum of Squared Level (RSS)", Skewness and Kurtosis. They are computed as follows.

Mean: Mean is computed over the window B having the size of $w \times w$, as

$$\mu = \frac{1}{w \times w} \sum_{i=1}^{w \times w} p_i \quad \ldots (17)$$

where, p_i is the intensity of pixel at i^{th} location in a window.

Maximum: Maximum feature in the given window, is calculated as

$$Mx = Max(B) \quad \ldots (18)$$

Minimum: The minimum feature in the given window, is calculated as

$$Mn = Min(B) \quad \ldots (19)$$

Standard deviation: This statistical metric explores the relative distribution of a pixel through statistical mean. It is termed as variance of the square root. Standard Deviation is computed as follows;

$$\sigma = \sqrt{\frac{1}{w \times w} \sum_{i=1}^{w \times w} (p_i - \mu)^2} \quad \ldots (20)$$

Mean Absolute Deviation (MAD): It explores the variability of Information for a given window. Mathematically, it is expressed as

$$MAD = \frac{1}{w \times w} \sum_{i=1}^{w \times w} (p_i - \mu) \quad \ldots (21)$$

Root Sum of Squared Level: The connected components distribution is explored by RSS where square root is applied after each pixel's intensity has been squared and summed. The Mathematical expression for, RSS is given as

$$RSS = \sqrt{\frac{1}{w \times w} \sum_{i=1}^{w \times w} (p_i)^2} \quad \ldots (22)$$

Skewness: Asymmetry of data is determined by Skewness and is mathematically represented as

$$S = \frac{\mu^3}{\sigma^3} \quad \ldots (23)$$

Kurtosis

The tails of distributions of pixel intensity is explored by kurtosis, and is mathematically represented as follows.

$$K = \frac{\mu_4}{\sigma^4} \quad \ldots (24)$$

Morphological Features: For image segmentation, one of the popularly used methods is Mathematical Morphology (MM). The MM employs erosion and dilation as two operators. The linked objects are separated by Erosion operation which diminishes them and widens the holes. Dilation fills the holes there by it connects the objects in image. Morphological opening is achieved by applying erosion operation followed by dilation operation and morphological closing is achieved by applying dilation operation followed by erosion operation. Structuring Element (SE) is required to perform mathematical morphological operation and it depends on the object's shape and structure. SE is located on the image to locate the center pixel. Top-hat and bottom-hat transforms are used to extract mathematical morphology features. These two methods perfectly differentiate between background and vessel pixels. Darker regions are determined through bottom hat while bright regions are determined through top hat transform. The mathematical expressions are given as follows;

$$T_H(C) = C - (C \circ SE) \quad \ldots (25)$$

and

$$B_H(C) = (C \cdot SE) - C \quad \ldots (26)$$

Opening operation is denoted by ° and · means closing operation. SE has width of one pixel and length of 15 pixels.

Edge Features: Edges are considered as high frequency regions which determine the sudden changes in pixel intensities. Here, the minor vessels are different from background and hence they are treated as edge features. Towards the computation of edge features, different filters are available. Here, the proposed approach used five types of filters namely Laplacian of Gaussian (LoG), Canny, Sobel, Prewitt, and Roberts. Let's assume the reponses of five filters as $E_R(i,j)$, $E_P(i,j)$, $E_S(i,j)$, $E_C(i,j)$ and $E_L(i,j)$, the final feature is computed as

$$F_C(i,j) = \sum E_R(i,j) + E_P(i,j) + E_S(i,j) + E_C(i,j) + EL(i,j) \quad \ldots (27)$$

Each pixel's Fused Edge feature is represented as $F_C(i,j)$. Majorly, the benefits of using the five edge filters are as mentioned below;

- Roberts filter explores the edge information as specified by the high frequency range by computing the gradient value.
- Prewitt operator determines the difference in pixel intensities along both x-direction and y- direction.
- Sobel operator considers the pixels that have similar intensity as the center pixel in the mask. It's operation is similar to Prewitt operator.
- Canny operator fixes the corner points those are determined based on the gradients in three directions namely vertical, horizontal, and diagonal. It is a powerful edge operator.
- LoG removes unnecessary regions in the minor vessel image which are due to the presence of noise.

Classification of Minor Blood Vessels

Once every pixel of resultant image is described through different features, a final vector of size 18-D is formulated by concatenating them. Next, SVM is used to perform classification which is regarded as a binary classifier. It classifies every pixel into either vessel or background class. The most popular "Radial Basis Function (RBF)" is used in SVM.

Post Processing

After the classification, the output image is represented as M', which has classified pixels. During post processing, to get the complete vascular structure of retinal vessels the major blood vessel image M and M' are fused. Here, union operator is employed for fusion purpose and the result is the final vessel image. Mathematically it can be represented as

$$M_F = M \cup M' \quad \ldots (28)$$

where, M_F is the final retinal vessel image which is comprised of both minor and major vessels.

Simulation Results

A personal computer with capacity of 1 TB HD and 4 GB RAM having MATLAB tool was used for simulation. Various kinds of fundus images were used for analysis and the performance of the proposed method was determined by measuring different performance metrics. The results obtained were then compared.

Datasets

DRIVE dataset[26] holds 40 fundus images which are clubbed into two different categories named as training and testing, with each category containing 20 images. "Canon CR5 non-mydriatic 3CCD camera" having the "Field of View (FOV)" 45° was used to obtain all the fundus images. The fundus images have a spatial resolution of 565×584 pixels. These fundus images were used for experimental validation. DRIVE dataset also contains fundus images called as Ground-truth images that are manually segmented by medical experts. The manually segmented images are then segmented by two different observers to enable viewing in two distinct perspectives. These images are then referred for evaluating the method's performance. The segmented results obtained using DRIVE dataset by proposed method are exposed in Fig. 2.

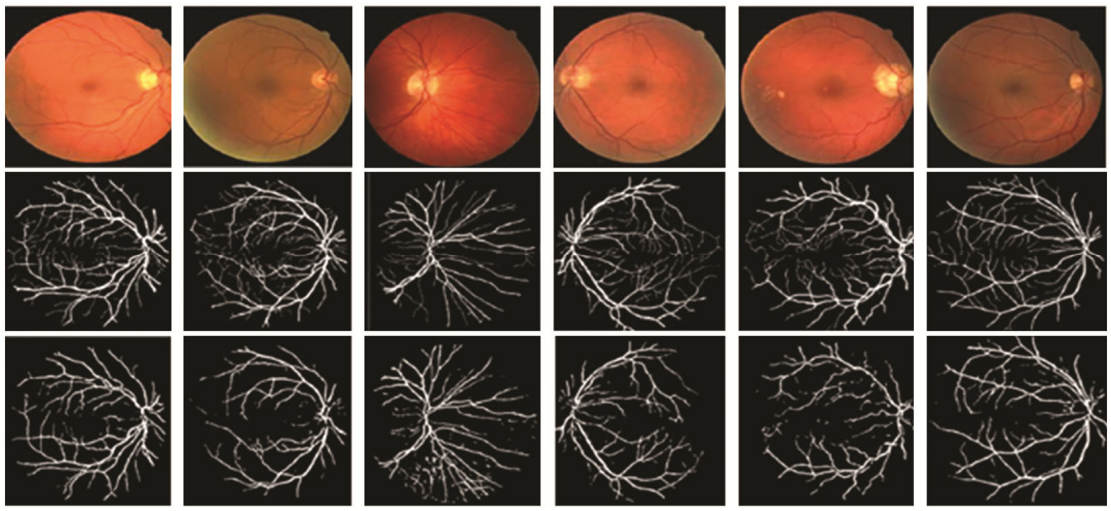

Fig. 2 — Results over the images of DRIVE, 1st row indicates RGB retinal fundus images, 2nd row indicates ground truth data and 3rd row indicates the retinal vessel structure derived through proposed approach.

Performance Metrics

Further, for subjective analysis, accuracy, specificity (precision), and sensitivity (true positive rate) were measured. In our work, A is considered as ground truth image and B as the segmented vasculature image and they are processed for assessment in their binary form only. The proposed segmentation approach is evaluated using DRIVE dataset and the obtained results are displayed in Table 1. It is noticed that the maximum sensitivity is 0.9141 and it is obtained over '06_test' image as shown in Table 1. Next, the minimum sensitivity is observed as 0.7119 and it is obtained over '15_test' image. Next, the maximum and minimum specificities are observed at 15_test image and 06_test image respectively. The maximum Accuracy of 0.9790 is observed at 19_test image and minimum accuracy is observed at 02_test image as it is of 0.9550. The maximum Jaccard index and Dice index are observed at 19_test image while the minimum Jaccard index and Dice Index at 08_test image. Among the 20 images, the 06_test image has taken less time for segmentation and 12_test image has taken more time for segmentation. The average values of sensitivity, specificity, accuracy, Jaccard index, Dice index and Time are observed as 0.8945, 0.9785, 0.9692, 0.6183, 0.7669, and 18.0856 sec respectively.

Table 1 — Performance analysis over DRIVE dataset through different metrics

Image	Sensitivity	Specificity	Accuracy	Jaccard Index	Dice Index	Time (Sec)
S1	0.8115	0.9844	0.9706	0.6505	0.7916	17.0838
S2	0.8825	0.9809	0.9550	0.6953	0.8238	17.1166
S3	0.8659	0.9713	0.9640	0.6063	0.7581	18.8065
S4	0.8893	0.9785	0.9729	0.6546	0.7947	17.9955
S5	0.9010	0.9729	0.9689	0.6167	0.7663	19.3371
S6	0.9141	0.9670	0.9645	0.5829	0.7397	16.4389
S7	0.8677	0.9756	0.9688	0.6167	0.7662	17.7215
S8	0.8673	0.9715	0.9661	0.5608	0.7217	16.6387
S9	0.9058	0.9736	0.9709	0.5749	0.7333	18.0591
S10	0.8592	0.9792	0.9722	0.6150	0.7649	16.5691
S11	0.8246	0.9795	0.9683	0.6208	0.7694	17.9513
S12	0.8571	0.9776	0.9743	0.6132	0.7636	19.5436
S13	0.8893	0.9702	0.9653	0.6017	0.7546	19.2021
S14	0.7759	0.9862	0.9702	0.6236	0.7715	19.3141
S15	0.7119	0.9909	0.9693	0.5979	0.7516	18.9654
S16	0.8695	0.9785	0.9714	0.6393	0.7833	17.1434
S17	0.8562	0.9743	0.9678	0.5756	0.7338	18.9140
S18	0.7909	0.9825	0.9696	0.5987	0.7522	18.6162
S19	0.8415	0.9900	0.9790	0.7018	0.8284	19.0767
S20	0.8093	0.9855	0.9747	0.6199	0.7687	17.2176

The performance comparative analysis between the earlier and developed methodologies through different performance metrics is shown in Table 2. For the comparison purpose, the methods that used DRIVE and STARE datasets for simulation experiments were referred. From the comparison, it is found that the maximum sensitivity is observed for Orujov *et al.*[17] on STARE dataset while the maximum sensitivity is observed for proposed methods on DRIVE dataset. However, the maximum specificity is observed for proposed method for both datasets. The maximum accuracy is observed as 0.9638 and it is gained by Yan *et al.*[11] on the STARE dataset while the maximum accuracy is gained by proposed method on DRIVE dataset and it is approximately 0.9621. Further, for the CHASE_DB also the proposed method gained better performance. The maximum accuracy is attained as 0.9568 and maximum sensitivity and specificity are observed as 0.8012 and 0.9766 respectively. The most important thing observed is that the proposed method required very less computational time when compared to the existing methods. Since the proposed method focused only on the minor vessels for training, computation time has reduced for both training and testing.

Table 2 — Performance comparison on different datasets

Author	Dataset	Sensitivity	Specificity	Accuracy	Time
Dash *et al.*[10]	DRIVE	0.7190	0.9760	0.9555	1.66 Sec
Yan *et al.*[11]	DRIVE	0.7631	0.9820	0.9538	—
Sazak *et al.*[12]	DRIVE	0.7180	0.9810	0.9590	3.8 Sec
Khan *et al.*[13]	DRIVE	0.7696	0.9651	0.9506	18 Sec
Lin *et al.*[14]	DRIVE	0.7632	—	0.9506	12 Hours for Training and 0.3 Sec for testing
Tamim *et al.*[15]	DRIVE	0.7542	0.9843	0.9607	—
Kushol *et al.*[16]	DRIVE	0.7588	0.9748	0.9456	—
Orujov *et al.*[17]	DRIVE	0.8380	0.9570	0.9390	1010 milliseconds on an average
Shukla *et al.*[18]	DRIVE	0.7015	0.9836	0.9476	—
Tehinda *et al.*[19]	DRIVE	0.7352	0.9775	0.9480	—
Dikkala *et al.*[20]	DRIVE	0.6340	0.9803	0.9476	30 Approximately
Proposed	DRIVE	0.8412	0.9866	0.9621	10 Min for Training and 1.5 Sec for testing

Training or testing partial portion of image results in less computation time when compared to that of the whole image. Moreover, the suggested method employed simple mathematical morphology operation which has less computational complexity.

Conclusions

This paper proposed a novel approach for the segmentation of retinal blood vasculature from retinal images through morphology, cascade features and supervised learning. The proposed method segmented both minor and major vessels which are more important attributes especially for the advanced stages of DR, i.e., proliferative DR. Most of the earlier methods failed at the extraction of complete vascular structure especially the extraction of minor vessels. The main reason is that the minor vessels are analogous to background pixels. This method differentiates them and hence extracted almost entire vessels with more accuracy. Three datasets were used for the purpose of simulation, and performance parameters used are sensitivity, specificity, accuracy and time computation were measured to determine their performance. Along with an improvement in the segmentation performance, the proposed method had shown outstanding performance in reducing computation time.

References

1 Xu L, Wang Y, Li Y, Wang Y, Cui T, Li J & Jonas J B, Causes of blindness and visual impairment in urban and rural areas in Beijing: the Beijing eye study, *Ophthalmology*, **113(7)** (2006) 1134, doi: 10.1016/j.ophtha.2006.01.035.

2 Congdon N, Zheng Y & He M, The worldwide epidemic of diabetic retinopathy, *Indian J Ophthalmol*, **60(5)** (2012) 428–431, doi: 10.4103/0301-4738.100542.

3 Yau J W Y, Rogers S L, Kawasaki R, Lamoureux E L, Kowalski J W, Bek T, Chen S J, Dekker J M, Fletcher A, Grauslund J, Haffner S, Hamman R F, Ikram M K, Kayama T, Klein B E K, Klein R, Krishnaiah S, Mayurasakorn K, O'Hare J P, Orchard T J, Porta M, Rema M, Roy M S, Sharma T, Shaw J, Taylor H, Tielsch J M, Varma R, Wang J J, Wang N, West S, Xu L, Yasuda M, Zhang X, Mitchell P & Wong T Y, Global prevalence and major risk factors of diabetic retinopathy, *Diab Care*, **35(3)** (2012) 556–564, doi: 10.2337/dc11-1909.

4 Candrilli S D, Davis K L, Kan H J, Lucero M A & Rousculp M D, Prevalence and the associated burden of illness of symptoms of diabetic peripheral neuropathy and diabetic retinopathy, *J Diabetes Complications*, **21(5)** (2007) 306–314, doi: 10.1016/j.jdiacomp.2006.08.002.

5 Roychowdhury S, Koozekanani D D & Parhi K K, Screening fundus images for diabetic retinopathy, *Proc Forty Sixth Asilomar Conference on Signals, Systems and Computers* (IEEE) 2012, 1641–1645, doi: 10.1109/ACSSC.2012.6489310.

6 Roychowdhury S, Koozekanani D & Parhi K, Dream: Diabetic retinopathy analysis using machine learning, *IEEE J Biomed Health Inform*, **18(5)** (2013) 1717–1728, doi: 10.1109/JBHI.2013.2294635.

7 Perfetti R, Ricci E, Casali D & Costantini G, Cellular neural networks with virtual template expansion for retinal vessel segmentation, *IEEE Transactions on Circuits and Systems II: Express Briefs*, **54(2)** (2007) 141–145, doi: 10.1109/TCSII.2006.886244.

8 Kovács G & Hajdu A, A self-calibrating approach for the segmentation of retinal vessels by template matching and contour reconstruction, *Med Image Anal*, **29(9)** (2016) 24–46, doi: 10.1016/j.media.2015.12.003.

9 Zhu C, Zou B, Zhao R, Cui J, Duan X, Chen Z & Liang Y, Retinal vessel segmentation in colour fundus images using extreme learning machine, *Comput Med Imaging Graph*, **55** (2017) 68–77, doi: 10.1016/j.compmedimag.2016.05.004.

10 Dash J & Bhoi N, A thresholding based technique to extract retinal blood vessels from fundus images, *Future Computing Inform J*, **2(2)** (2017) 103–109, doi: 10.1016/j.fcij.2017.10.001.

11 Yan Z, Yang X & Cheng K, A three-stage deep learning model for accurate retinal vessel segmentation, *IEEE J Biomed Health Inform*, **23(4)** (2019) 1427–1436, doi: 10.1109/JBHI.2018.2872813.

12 Sazak Ç, Nelson C J & Obara B, The multiscale bowler-hat transform for blood vessel enhancement in retinal images, *Pattern Recognition*, **88** (2019) 739–750, https://doi.org/10.1016/j.patcog.2018.10.011.

13 Khan M A U, Carmichael J N, Sarirete A & Mir N, Thin vessel detection and thick vessel edge enhancement to boost performance of retinal vessel extraction methods, *Procedia Comput Sci*, **163** (2019) 618–638, doi: 10.1016/j.procs.2019.12.144.

14 Lin Y, Zhang H & Hu G, Automatic retinal vessel segmentation via deeply supervised and smoothly regularized network, *IEEE Access*, **7** (2019) 57717–57729, doi: 10.1109/ACCESS.2018.2844861.

15 Tamim N, Elshrkawey M, Azim G A & Nassar H, Retinal blood vessel segmentation using hybrid features and multi-layer perceptron neural networks, *Symmetry (Basel)*, **12(6)** (2020) 894, https://doi.org/10.3390/sym12060894.

16 Kushol R, Kabir M H, Abdullah-Al-Wadud M & Islam M S, Retinal blood vessel segmentation from fundus image using an efficient multiscale directional representation technique bendlets, *Math Biosci Eng*, **17(6)** (2020) 7751–7771, doi: 10.3934/mbe.2020394.

17 Orujov F, Maskeliunas R, Damaˇseviˇcius R & Wei W, Fuzzy based image edge detection algorithm for blood vessel detection in retinal images, *Appl Soft Comput J*, **94** (2020) 106452, doi: 10.1016/j.asoc.2020.106452.

18 Shukla A K, Pandey R K & Pachori R B, A fractional filter based efficient algorithm for retinal blood vessel segmentation, *Biomed Signal Process Control*, **59(7)** (2020) 101883, doi: 10.1016/j.bspc.2020.101883.

19 Tchinda B S, Tchiotsop D, Noubom M, Louis-Dorr V & Wolf D, Retinal blood vessels segmentation using classical edge detection filters and the neural network, *Inform Med Unlocked*, **23(3)** (2021) 100521, doi: 10.1016/j.imu.2021.100521.

20 Dikkala U, Joseph M K & Alagirisamy M, A comprehensive analysis of morphological process dependent retinal blood vessel segmentation, *Proc International Conference on Computing, Communication, and Intelligent Systems* (IEEE) 2021, 510–516, doi: 10.1109/ICCCIS51004.2021.9397095.

21 Devi Y A S & Kamsali M C, Retinal image contrast enhancement through pixel collaboration in spatial domain, *Int J Intell Eng Syst*, **15(3)** (2022) 500–514, doi: 10.22266/ijies2022.0630.42.

22 Roychowdhury S, Koozekanani D D & Parhi K K, Blood vessel segmentation of fundus images by major vessel extraction and subimage classification, *IEEE J Biomed Health Inform*, **19(3)** (2015) 1118–1128, doi: 10.1109/JBHI.2014.2335617.

23 Frame A, Undrill P, Cree M, Olson J, McHardy K, Sharp P & Forrester J, A comparison of computer based classification methods applied to the detection of microaneurysms in ophthalmic fluorescein angiograms, *Comput Biol Med*, **28** (1998) 225–238, doi: 10.1016/s0010-4825(98)00011-0.

24 Fraz M, Remagnino P, Hoppe A, Uyyanonvara B, Rudnicka A, Owen C & Barman S, An ensemble classification-based approach applied to retinal blood vessel segmentation, *IEEE Trans Biomed Eng*, **59(9)** (2012) 2538–2548, https://doi.org/10.1109/tbme.2012.2205687.

25 Fraz M M, Barman S A, Remagnino P, Hoppe A, Basit A, Uyyanonvara B, Rudnicka A R & Owen C G, An approach to localize the retinal blood vessels using bit planes and centerline detection, *Comput Methods Programs Biomed*, **108(2)** (2012) 600–616, doi: 10.1016/j.cmpb.2011.08.009.

26 Staal J, Abramoff M, Niemeijer M, Viergever M & van Ginneken B, Ridge-based vessel segmentation in color images of the retina, *IEEE Trans Med Imaging*, **23(4)** (2004) 501–509, doi: 10.1109/TMI.2004.825627.